Field Crops Research 309 (2024) 109332

Contents lists available at ScienceDirect

Field Crops Research

journal homepage: www.elsevier.com/locate/fcr

Usefulness of techniques to measure and model crop growth and yield at different spatial scales

Di He [a,*], Enli Wang [a], John Kirkegaard [a], Eusun Han [a,b,c], Brendan Malone [a], Tony Swan [a], Stuart Brown [a], Mark Glover [a], Roger Lawes [d], Julianne Lilley [a]

[a] CSIRO Agriculture and Food, GPO Box 1700, Canberra, ACT 2601, Australia
[b] University of Copenhagen, Department of Plant and Environmental Sciences, Taastrup 2630, Denmark
[c] Aarhus University, Department of Agroecology, Tjele 8830, Denmark
[d] CSIRO Agriculture and Food, 147 Underwood Avenue, Floreat, WA 6014, Australia

ARTICLE INFO

Keywords:
Ground measurement
Yield map
Remote sensing
Drone
APSIM
Yield variability

ABSTRACT

Context: Within-field yield variability affects crop production and management decisions. To understand and manage this variability, different techniques have been deployed to measure and monitor the crops (and soils) at various spatial scales, including manual measurements, harvester-mounted yield monitors, proximal and remote sensing and crop simulation modelling. The value of this increasing data availability to enhance process understanding and on-ground management is unclear.

Objective: This study aimed to investigate the value of the increasingly available spatial data from different sources to understand important soil-plant processes amenable to improvement in both simulation modelling and for better management decisions for dryland cropping.

Methods: We collected three types of measurement data (manual sampling, sensed data from satellite and drone, and yield maps) over a 10 ha field and conducted simulations using the process-based soil-plant model APSIM at different spatial scales (varied from 1 m^2 up to 10 ha). We assessed the agreement between ground measurements and yield maps, analysed the potential to use remotely sensed vegetation indices to estimate yield, and the scale at which process-based modelling could be reliable.

Results: Wheat yield extracted from yield map at 1 m^2 spatial resolution only explained 30% of the variation in yield measured from 1 m^2 manual sampling, with better agreement when data was aggregated to 1 ha strip-scale ($R^2 = 0.66$, NRMSE = 9.1%). Remotely sensed vegetation indices (VI) were better correlated with the yield map when aggregating images to coarse spatial resolution (> 50 m × 50 m), while high-resolution drone VI increased the correlation at finer scales. However, the relationship and the timing of the highest correlation differed between years. APSIM simulated point-based yield measured from manual samples with NRMSE of 19.4%, but it was difficult to capture spatial variation in yield due largely to uncertainties in input data. However, APSIM simulations captured the average crop growth dynamics and yield well at 1 ha strip- and 10 ha whole field scales.

Conclusions: The results highlight the need for caution when using yield maps and remote sensing data to quantify spatial variability and inform spatially explicit management decisions at a fine resolution (e.g., 1 m^2). In our case, remote sensing data and yield maps only became consistent and process-based modelling became skilful at scales larger than a 1 ha strip.

Implications: Despite an increasing amount of high-resolution spatial data, the usefulness at fine resolution needs further investigation, particularly under heterogeneous field conditions. Such data need to be analysed in conjunction with the landscape, soil and climate data to understand the drivers of spatial variability and inform process understanding and modelling. This further implies potential problems in developing spatial management practices at finer scales using such data.

* Corresponding author.
E-mail address: di.he@csiro.au (D. He).

https://doi.org/10.1016/j.fcr.2024.109332
Received 14 August 2023; Received in revised form 29 February 2024; Accepted 3 March 2024
Available online 10 March 2024

1. Introduction

Quantification of yield variation within fields is essential to understanding the key biophysical drivers of the spatial variation underpinning crop growth and yield, which is fundamental to effective crop management and resource allocation. With the advances in digital soil and plant sensors, earth observation and mapping technologies, crop canopy characteristics, crop yields, soil attributes and their changes can now be sensed and mapped over different spatial and temporal scales (Godwin and Miller, 2003; Schuster et al., 2023). The spatial resolutions and the accuracy of such data vary with the technology used, causing potential problems in using the data to analyse crop performance and inform farm management.

Manual measurements such as in-season crop biomass and soil sampling are regarded as a gold standard to describe soil and plant properties for a given sampling area. However, the representativeness of sample-based results for larger areas (upscaling) limits the extrapolation of manual measurements to describe within-field spatial variability of crop growth and yield at different scales (Jordan et al., 2003; Kosmowski et al., 2021). Yield monitoring and mapping is by far the quickest and most convenient way to both collect and document yield and its spatial variability (Kharel et al., 2019). Yield maps generated from yield monitoring are valuable sources of spatial data for precision agriculture. Yield monitors are often calibrated against a reference yield, but the level of agreement between ground measurements and yield maps across various spatial scales has not received sufficient enquiry.

The high spatial and temporal resolution of sensors onboard spaceborne platforms are being used to build a new generation of agricultural monitoring systems (Skakun et al., 2021). Several approaches have been developed to estimate or forecast crop yield from remote sensing data, including i) establishing an empirical relationship between yields and vegetation indices (VI) or metrics derived from VI time series (Hu et al., 2021; Skakun et al., 2021), ii) assimilation of remote sensing data into process-based models (Campos et al., 2019; Jin et al., 2018), and iii) calibration-free approaches which develop empirical models with process-based model simulation results without reliance on ground measurements (Deines et al., 2021; Lobell et al., 2015). For all those methods, the correlation between VI and yield at different spatial resolutions is the basic indicator of estimation/prediction potential. If VI is well correlated with yield at a given scale, the VI should have great potential to estimate yield and its spatial variability. However, there is often a lack of ground-truthing data at matching resolutions.

Agricultural systems modelling integrates measured data with underpinning biological and physical processes to simulate the dynamic changes in crop growth and soil conditions in response to climate and management, and how they interact to determine productivity and sustainability outcomes (Holzworth et al., 2014; Keating et al., 2003). More recently, process-based modelling has been used with new data layers from advanced technologies such as remote sensing, to fill data gaps in both spatial and temporal dimensions, to disentangle the impacts of confounding drivers and processes, and to predict crop and soil attributes that are difficult to measure. Examples include prediction of within-field crop yield and its variability (Gaso et al., 2021; Maestrini and Basso, 2018; Ziliani et al., 2022), establishment of temporal and spatial relationships between yield and remote/proximal sensed imagery (Skakun et al., 2021; Zarco-Tejada et al., 2005), analysis of the effects of climate variability and resource management on the spatial pattern of yield (Batchelor et al., 2002; Huggins and Alderfer, 1995; Robertson et al., 2008), identification of causes for crop yield variability (Boenecke et al., 2018; Bölenius et al., 2017; Jones et al., 2022), and prediction of variations in soil properties from crop yields using an inverse modelling approach (He et al., 2022, 2021).

However, questions remain regarding how well the data and simulation results capture spatial heterogeneity across the field, particularly for data acquired from a heterogeneous field for process-based modelling that requires a significant amount of input data. In this paper, we select a typical 10 ha field at CSIRO's Boorowa Agricultural Research Station in the wheatbelt of Australia and use three types of measured data, i.e., manual sampling, remote sensing (satellite and drone-based), yield maps, and soil-plant modelling with the farming systems model APSIM (Holzworth et al., 2014) to investigate the relationships and reliability of data collected at different scales by different technologies, including 1) The agreement between point-based manual measurements and yield maps at different spatial scales; 2) The possibilities of using vegetation index (NDVI) from satellite and drone imagery to predict within-field yield at different scales; 3) The scale at which process-based soil-crop modelling can be reliably used to augment the data and enhance process understanding.

2. Material and Method

2.1. The study site

The CSIRO Boorowa Agricultural Research Station (BARS, 290 ha) is a state-of-the-art agricultural research facility near the town of Boorowa in southern New South Wales, Australia. The Boorowa region is a grazing and cropping region, where the average annual rainfall (1970 – 2021) is 645 mm and the annual average temperature is 13.6 °C. This study used a dataset collected from a long-term trial (LTT) established in a 10 ha field (450 m × 220 m, LTT) with 8 strips (each 450 m × 24 m) at BARS from 2019 and 2021 (Fig. 1). The annual rainfall at BARS in 2019, 2020 and 2021 was 481 mm, 782 mm and 909 mm, respectively. The crops grown in the LTT field were winter wheat (cultivar *Kittyhawk*) sown on 10 April 2019, Timok Vetch sown on 25 April 2020 (terminated for brown manure) and spring wheat (cultivar *Rockstar*) sown on 13 May 2021. Total fertiliser nitrogen input on wheat was 88.2 kg N/ha in 2019 and 133.2 kg N/ha in 2021. Detailed management information was recorded including tillage, seeding rate, sowing and harvest dates, dates and amount of fertilizer applications, pesticide and herbicide applications since 2016 (Table S1).

The common soil types following the Australian Soil Classification (Isbell, 2021) at BARS are Yellow or Red Chromosols or Kurosols depending on the presence of subsoil acidity. The elevation across BARS ranges from 490 m to 560 m above sea level and decreases from west to southeast. For the LTT field, there are undulating rises across the field. pH stratification phenomenon occurs between 5 and 30 cm (pH < 5), where there is a clear decrease in soil pH from 5 to 30 cm and then an increase from 30 cm to deeper layers (Malone et al., 2022).

2.2. Soil data

A suite of 3D digital soil attribute maps were available for BARS including pH, soil organic carbon, cation exchange capacity (CEC), texture, whole soil bulk density, and soil water holding characteristics, namely crop lower limit (CLL) and drained upper limit (DUL) as per Coughlan et al. (2002). The digital soil mapping models were constructed using the data collected through farm-wide on-the-go proximal soil sensing, soil sampling, and soil core scanning (visible and near-infrared spectrometry (visNIR) and gamma attenuation) (Figure S1). Details can be found in Malone et al. (2022). There are 30 soil moisture sensors installed in the LTT field (Fig. 1a) to measure soil temperature and soil water content at 20 cm intervals down to 180 cm depth. The sensors were positioned with the dual purposes of geographical and soil-landscape information coverage. For geographical coverage, the one requirement was to have at least 3 sensors situated in each experimental strip. For soil-landscape information coverage, the conditioned Latin Hypercube sampling (cLHS; Minasny and McBratney, 2006) algorithm was used. Input into the cLHS algorithm was the suite of digital soil and environmental mapping derived in Malone et al. (2022). Effectively a multi-dimensional data cube that the algorithm is designed to process through, cLHS ensures a balanced selection of sites across feature or data space ensuring spatial variability is covered in an

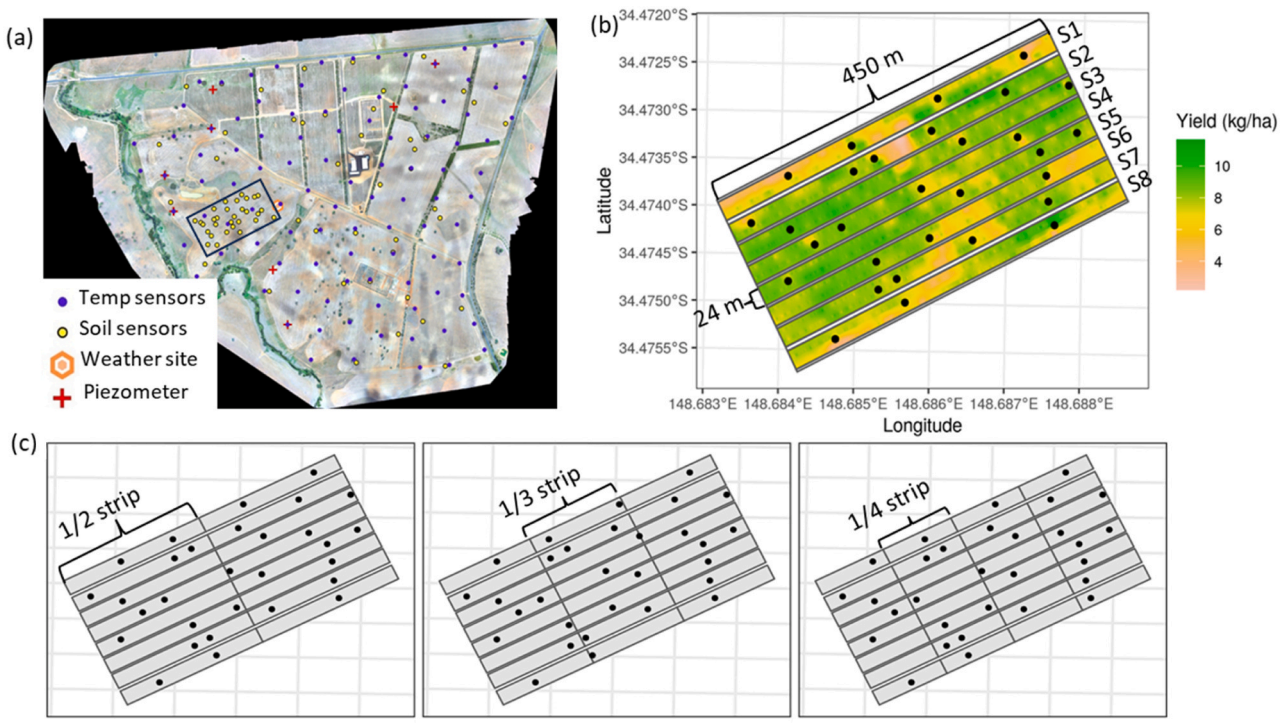

Fig. 1. The CSIRO Boorowa Agricultural Research Station (BARS), Australia (a) and the wheat yield map of the study field (black rectangle in panel a) in 2021 (b). S1 - S8 in panel (b) indicate strip 1 to strip 8. Each strip was split into 1/2 strip, 1/3 strip and 1/4 strip to create different spatial extent for evaluating the usefulness of techniques to measure crop yield, and panel (c) shows the diagram. The black dots in (b) and (c) show manual crop sampling points (in 2021) which are around the soil moisture sensors in panel (a).

optimal way with the number of available sensors to be installed. A further nuanced spatial analysis was performed to ensure placement of sensors occurred outside of fixed machinery track lines. Processed soil moisture data has been updated in real-time on Senaps (https://senaps.io/dashboard/#/app/group/detail/boorowa-soil-analytics) since Jul 2019.

In 2021, soil samples were taken around the 30 soil sensors (Fig. 1) to measure mineral nitrogen and soil water contents before sowing. Soil cores were taken up to 155 cm in deep and 90 cm in shallow soils. Cores were cut into 5 cm intervals for the top layers (0 – 20 cm) and 20 cm intervals for the subsoil. The mineral nitrogen was extracted in 0.5 M KCl (50 g:100 mL). Ammonium and nitrate contents were determined by continuous flow colourimetry, using the Griess–Ilosvay and the indophenol methods (Stock, 1983).

2.3. Crop data

In 2021, the crop was sampled manually around each of the 30 soil moisture sensors (Fig. 1, at least 2 m away from sensors to avoid any impact on sensor reading but close enough to be similar to the crop on the sensor) according to the developmental stages described in Zadoks (Zadoks et al., 1974). Plants were cut at ground level from a 1.2 m × 1 m quadrat at wheat stem elongation (Zadok 30, 20 Aug 2021), flag leaf (Zadok 39, 6 Oct 2021), and anthesis (Zadok 60, 28 Oct 2021) stage. Biomass was determined after oven-drying the samples at 70° C for 48 hours. Prior to drying, leaf area index (LAI) was measured using Li-3100 area meter (Li-COR, inc. USA) for a sub-sample of 25 tillers. Final sampling was collected on 14 Dec 2021 and biomass, grain yield, yield components and protein were measured.

In 2019 and 2021, wheat yield was collected using a calibrated yield monitor attached to a commercial grain harvester which cut 12 m x 1 m swathes of crop. The yield monitor is mounted on a combine harvester and measures in real-time the amount of grain that passes through the combine harvester when the crop is being harvested. The distance between adjacent passes is 12 m and the distance between the consecutive record is 1 m. The raw data was cleaned and interpolated to 1 m x 1 m spatial resolution yield maps following the protocol of PAT-Precision Agriculture Tools (Ratcliff et al., 2019) in R software. The basic steps are, (1) clipping the data to a given boundary; (2) cleaning data using 3 times standard deviation, i.e., filtering the values out of mean value ± 3 x standard deviations; (3) using ordinary kriging to interpolate the point data to 1 m x 1 m raster. Based on this, we assumed that an interpolated yield of a larger area around the manual sampling area could be equivalent to the manual sampling yield.

2.4. Remotely sensed data

Multispectral images from the two Sentinel-2 satellites (2 A and 2B) for the whole growing season of wheat crops in 2019 and 2021 were processed and downloaded via Google Earth Engine (COPERNICUS/S2_SR) (Gorelick et al., 2017). The cloud and shadows were masked, and the pixels with > 5% of cloud were filtered out. After processing, there were 39 and 23 high-quality images in 2019 and 2020 from April to December, respectively.

In 2021, a quadrotor UAV system, Phantom 4 Pro (DJI Inc., Shenzhen, China), mounted with a five-band (blue, green, red, red-edge, near-infrared) multi-spectral camera (Micasense RedEdge-M) was flown over the field covering 14.34 ha on five dates 08 Sep, 22 Sep, 6 Oct, 1 Nov and 29 Nov corresponding with wheat development stages of stem elongation (Zadok 35), flag leaf (Zadok 38), booting (Zadok 45), anthesis (Zadok 63), and grain filling (Zadok 80), respectively. The images were captured at 50 m altitude which resulted in the average ground sampling distance (GSD) of 4.24 cm per pixel. Radiometric corrections were performed using the reflectance panel for each flight campaign. Pix4D mapper software (Pix4D, S.A., Switzerland) was used for image stitching. Georeferencing was done using 21 pre-installed ground control points (GCPs) with known coordinates.

Normalised Difference Vegetation Index (NDVI) is a simple index

that measures the difference-sum ratio between near-infrared and red light reflected by plant leaves (Eq. 1), which is used to describe the canopy cover for spatial variations and temporal dynamics based on the fact that chlorophyll absorbs red whereas the mesophyll leaf structure scatters NIR (Pettorelli et al., 2005).

$$NDVI = (NIR - RED)/(NIR + RED) \quad (1)$$

where NIR and RED are the amounts of near-infrared and red light, respectively, reflected by the vegetation and captured by the sensors of the satellite and drone.

2.5. Yield from manual sampling and yield maps

We aimed to address two questions using this wheat yield dataset. The first question was whether wheat yield extracted from the yield mapping agreed with the yield measurements from manual sampling. The second question was whether point-based manual measurements can be used to estimate yield at different spatial scales, such as sub-strip, strip or multiple strips. To answer these questions, we compared the yield extracted from yield maps and manual sampling at different spatial scales. First, wheat yield extracted from a yield map was compared with manual measurements at 1 m x 1 m spatial scale. We used coordinates of the 30 soil moisture sensors to extract yield from the yield map to get the 1 m x 1 m yield data, then compared them with manual measurements. Then in order to create different spatial scales, each strip (8 strips in Fig. 1b) was split into 1/2 strip, 1/3 strip, and 1/4 strip (Fig. 1c). Two strips, 3 strips, 4 strips and 5 strips were created through 2-, 3-, 4- and 5-combinations of 8 strips (i.e., 28, 56, 70, 56 repetitions for 2, 3, 4, 5 strips, respectively). For a given target area, yield from the yield maps and manual sampling were calculated as the mean of that area. Normalized root mean square error (NRMSE) was used to assess the agreement between them and the regression-based coefficient of determination (R^2) was used to assess the correlation.

NRMSE was calculated as follows:

$$NRMSE = \sqrt{\sum_{i=1}^{n}(P_i - S_i)^2 \Big/ n} \Big/ \overline{S} \quad (2)$$

P_i is the manual measurement of yield and S_i is the wheat yield derived from the yield map, $\overline{S}$ is the average yield. R^2 was calculated directly in R software (R Core Team, 2022) with function lm(). lm() is a function to fit linear regression models.

The variability of yield was quantified using the coefficient of variation:

$$CV = \sigma/\mu \quad (3)$$

CV is the coefficient of variation, σ is the standard deviation and μ is the mean. σ was calculated directly in R software (R Core Team, 2022) with function sd().

2.6. Remotely sensed vegetation index and yield

Spatial correlation between remotely sensed vegetation index (VI) and crop yield is the basic indicator to assess the potential of using VI to estimate yield at different spatial scales. The NDVI is the most widely used index to estimate crop yield, which has been used to predict wheat yield at a within-field scale in the northern grain-growing region of Australia with moderate predictive accuracy (RMSE = 790 kg/ha) (Lai et al., 2018). Here correlation coefficients between NDVI and yield maps were calculated for each observation date at the original spatial resolution, i.e., 10 m x 10 m for Sentinel-2 imagery and 1 m x 1 m for drone imagery. The dates where the highest correlation coefficients emerged were pinpointed. The images of those dates (Sentinel-2: 6 Nov 2019 and 31 Oct 2021, drone: 1 Nov 2021) were used to calculate the correlation coefficients at different spatial scales or spatial extents of 10 m x 10 m, 20 m x 20 m, 30 m x 30 m, 40 m x 40 m, 1/4 strip, 1/3 strip, 1/2 strip and whole strip. The images were aggregated to 10 m (for drone images), 20 m, 30 m and 40 m using the function terra::aggregate() in R software (Hijmans et al., 2023). For the correlation coefficients at 1/4 strip, 1/3 strip, 1/2 strip and strip levels, the average of NDVI and yield from both maps for the given area were used. For drone images, as the original spatial resolution was 1 m x 1 m, we also calculated the correlation coefficients between NDVI and yield maps at spatial resolution higher than 10 m x 10 m, which was from 1 m x 1 m to 10 m x 10 m with 1 m interval.

Pearson correlation coefficient was calculated as follows:

$$r = \frac{\sum (x_i - \overline{x})(y_i - \overline{y})}{\sqrt{\sum (x_i - \overline{x})^2 \sum (y_i - \overline{y})^2}} \quad (4)$$

x_i is the value of NDVI at each grid cell or spatial extent, $\overline{x}$ is the mean of NDVI values. y_i is the value of yield at each grid or spatial extent, $\overline{y}$ is the mean of yield values. The basic function cor() in R software was used to calculate the Pearson correlation coefficients. The variability of NDVI was quantified by the coefficient of variation (Eq. 3).

2.7. Modelling crop growth and yield with APSIM

APSIM is a farming systems model that simulates crop development, biomass growth and grain yield at a daily time step in response to climatic and soil conditions and any management intervention (Holzworth et al., 2014). APSIM has been thoroughly tested across Australia for simulation of wheat phenology, biomass dynamics and yield (He and Wang, 2019; Zhao et al., 2022). The APSIM Classic Version 7.10 was used in this study to simulate the dynamics of soil water and nitrogen, wheat growth and yield in 2021.

The APSIM model was set up with the individual soil profiles at each of the 30 points in the LTT where soil sensors were located and manual crop measurements were made. Soil attributes of each point were extracted from the digital maps. The model was initialised with the initial soil water and mineral nitrogen measured at each soil depth in the 30 sites at the start of the season on 13 May 2021. Crop management was applied according to recorded sowing date, plant density, cultivar and fertilizer applications.

In addition, we also set up 9 additional APSIM runs, 8 for the 8 strips (Fig. 1b) using an average soil profile for each strip, and one for the entire 10 ha LTT field with an average whole field soil profile. For the 8 $\times$1 ha and entire 10 ha simulations, the soil profile data (i.e., bulk density, CLL, DUL, soil organic carbon, pH) were derived by averaging the data from the digital soil maps. The simulated wheat biomass dynamics and final yield were compared with the yield from the yield map and manual sampling to test the confidence of the spatially explicit point-based APSIM modelling. The range and variation of key functional soil properties for both point and strip scales are in Table 1.

The agreement between APSIM simulated yield and yield measured

Table 1
The value range, mean and coefficient of variation of key functional soil properties for APSIM.

Soil property	Spatial scale	Value range	Mean	CV
PAWC* (mm)	Point	119–206	177	14.1%
	Strip	153–193	179	8.4%
AWC** (mm)	Point	55–212	131	32.8%
	Strip	109–164	133	14.3%
Soil mineral N (kg/ha)	Point	65–230	124	34.7%
	Strip	85–147	133	15.0%

*PAWC is the plant available water holding capacity, i.e., the maximum amount of water held between crop lower limit and drained upper limit **AWC is the available water content for wheat at sowing. CV is the coefficient of variation.

from manual sampling or yield derived from yield maps was assessed by normalized root mean square error (NRMSE) and the regression-based coefficient of determination (R^2). The calculation method is like that in Section 2.5. The variability of simulated yield across the field was quantified using the coefficient of variation (Eq. 3).

3. Results

3.1. Agreement between manual measurements and yield maps

Based on the 30 manual samplings of wheat in 2021, wheat yield ranged from 5.3 to 10.0 t/ha. Yields derived from the yield map in 2021 had a slightly lower value ranging from 4.7 to 8.2 t/ha. The variability of the manually measured wheat yields was 16%, slightly larger than that for wheat yields from the yield map (12%). Both coefficients of variation are relatively small, similar to the average variation (13.3%) in wheat yields around the mean in field experiments (Taylor et al., 1999).

Wheat yields from the manual sampling (1 ×1.2 m^2) explained only 30% of the within-field variations reflected in the yield map in 2021 (R^2 = 0.30), with NRMSE of 20% (Fig. 2). Aggregating to the scale of a 1 ha strip, the average of the manual measurements explained 66% of the variation in strip-averaged yields from the yield maps (R^2 = 0.60), with a significantly reduced NRMSE of 9.1%. For the entire 10 ha field, the average of the 30 manual measurements was 8.29±1.34 t ha^{-1}, which is close to the average yield of 7.76±1.19 t ha^{-1} from the yield map. In general, the manual measurements of wheat yields were higher than those from yield maps. This may be due to mechanical harvesters being set up to discard small seeds that have no commercial value.

By splitting the field into equal rectangle areas (Fig. 1c), spatial extents with different sizes and containing different numbers of sampling points were created. The agreement between manually measured wheat yield and yield derived from yield maps at different spatial scales is shown in Fig. 3. When the spatial extent increased from 1/4 strip (0.25 ha) to a whole strip (1 ha), the R^2 increased from 0.29 to 0.66 and NRMSE declined from 15.0% to 9.1%. However, as the spatial extent further increased, both NRMSE and R^2 remained relatively constant. Results indicate that the average of manual measurements from 3 to 5 sampling points as replicates in the strip could adequately represent the yield variation at the strip scale. The representativeness of manual measurements at finer scales was significantly lower.

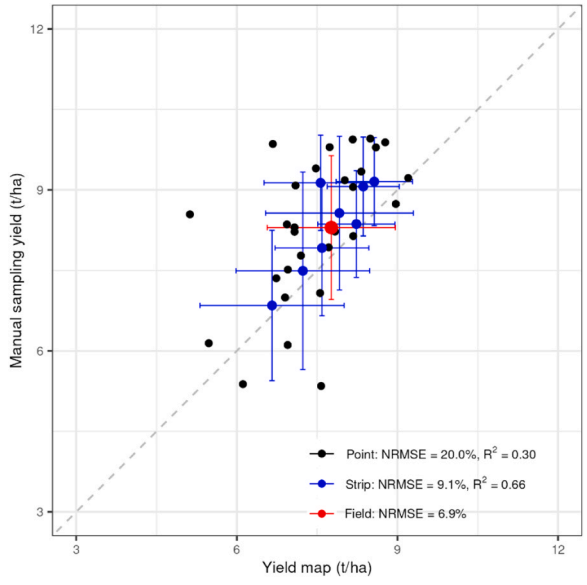

Fig. 2. Comparison of wheat yield from manual measurements and those from yield map at point, strip and field levels. NRMSE is the normalized root mean square error between manually measured yield and yield map. R^2 is the coefficient of determination. Error bars represent the standard deviation of wheat yields from manual sampling and yield map at the 30 sampling points.

3.2. Correlation between remotely sensed vegetation index and yield

The highest correlation between the spatial distribution of NDVI (maps) derived from Sentinel-2 images (10 m) and wheat yields derived from yield maps at the same spatial resolution was around 1 November for both years (Fig. 4), with the correlation coefficient of 0.66 and 0.61 in 2019 and 2021, respectively. NDVI maps derived from drone images in 2021 explained more variation in yield maps with the highest correlation coefficient of 0.81 around similar time (Fig. 4).

The higher spatial correlation between NDVI and wheat yields occurred at the later wheat development stage when NDVI declined. After NDVI reached the peak value, the correlation coefficient with yield increased and then decreased in both years. In 2019, the highest correlation value occurred at the mid-grain filling stage, while in 2021 it occurred just after flowering. The spatial correlation between NDVI and yields increased with increasing spatial extent (Fig. 5). When spatial resolution changed from 10 m to 50 m, the correlation coefficient increased from 0.65 to 0.81 in 2019 and from 0.61 to 0.63 in 2021. At strip level, the correlation coefficient between strip average NDVI and yields reached 0.96 and 0.82 in 2019 and 2021, respectively. The correlation between yield maps and NDVI maps derived from drone images followed a similar pattern of change in response to spatial scales.

3.3. Confidence of process-based modelling

For point-level simulations, APSIM simulated yields only explained around 2% of the variation in the yield map (Fig. 6a). However, the simulation error was relatively low compared to the yields on yield maps, with NRMSE = 13.3%. At strip-level, the averages of APSIM simulations only explained 6% spatial variation in yield map, but the simulation error reduced to an NRMSE of 7.8%. For the entire field, the average of APSIM simulated wheat yield was almost equal to the mean yield from yield map (Fig. 6a). Compared to the manual measurements at 1 m^2, APSIM simulation error was slightly higher than that derived from yield map. Simulation error was reduced when APSIM simulation changed from point-level to the whole field-level (Fig. 6b).

APSIM simulations captured the biomass dynamics relatively well at the strip level, except for a slight under-prediction for Strip 6, with simulation error of less than 10% for final biomass and yield (from both manually measured yields and yield maps) (Fig. 7). There was no significant difference in yield map average among strips (Fig. 6).

The variability of APSIM simulated final biomass and grain yields across strips (3% and 6%) was much smaller compared to those of the manual measurements (16%) and yields from yield map (12%). This is caused by the lack of variation in inputs of soil profile properties, e.g., spatial variability of PAWC was only 8% (153 mm – 192 mm), and that of initial mineral N content was 15% (85 kg N ha^{-1} – 147 kg N ha^{-1}) (Table 1).

4. Discussion

There is a significant discrepancy between the manually measured yield and yield extracted from the yield map at 1 m^2 scale. The R^2 value less than 0.3 suggests poor correlation between those two aspects. The RMSE greater than 20% signifies a substantial difference between those two measurements. Agreement between the two increased when point-measured yields were aggregated to larger scales, i.e., strips (1 ha) or whole field (10 ha). At 1 m^2 scale, the lack of correlation may be due to the inconsistent locations of the two (data was extracted from the yield map using the location of soil moisture sensors, while manual sampling was carried out around the sensors). Another possible reason is that the yield map was constructed by interpolation of point-scale data from the

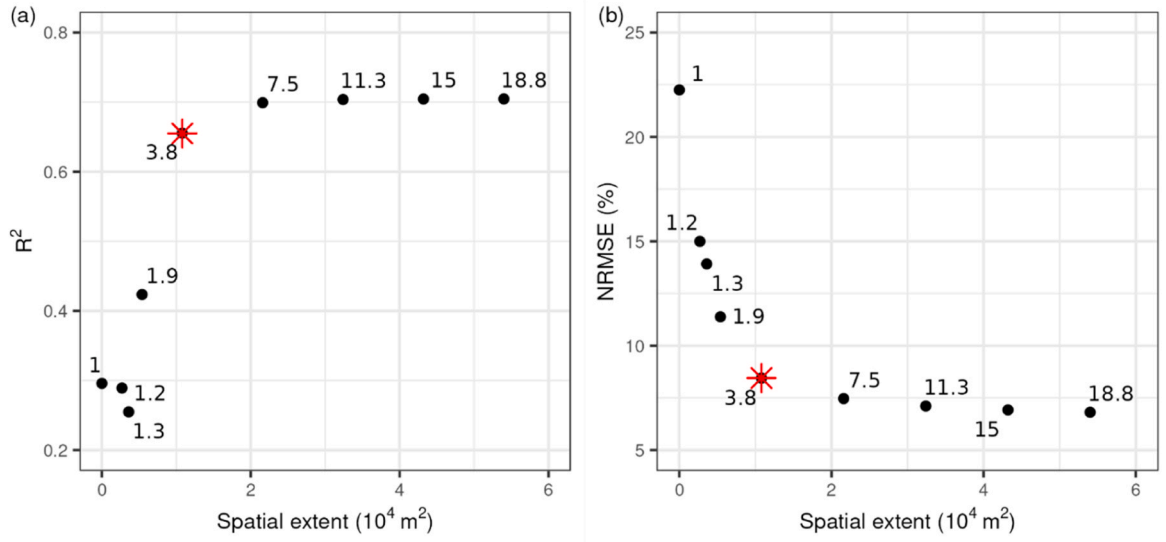

Fig. 3. Agreement between wheat yield derived from yield map and by manual measurements at different spatial scales (represented by the size of target areas) (a) and the corresponding NRMSE between the two (b). The red star indicates the value of strip level. NRMSE is the normalized root mean square error between manually measured yield and yield map. R^2 is the coefficient of determination. The number shows the sample size, i.e., the average number of points at each aggregation level.

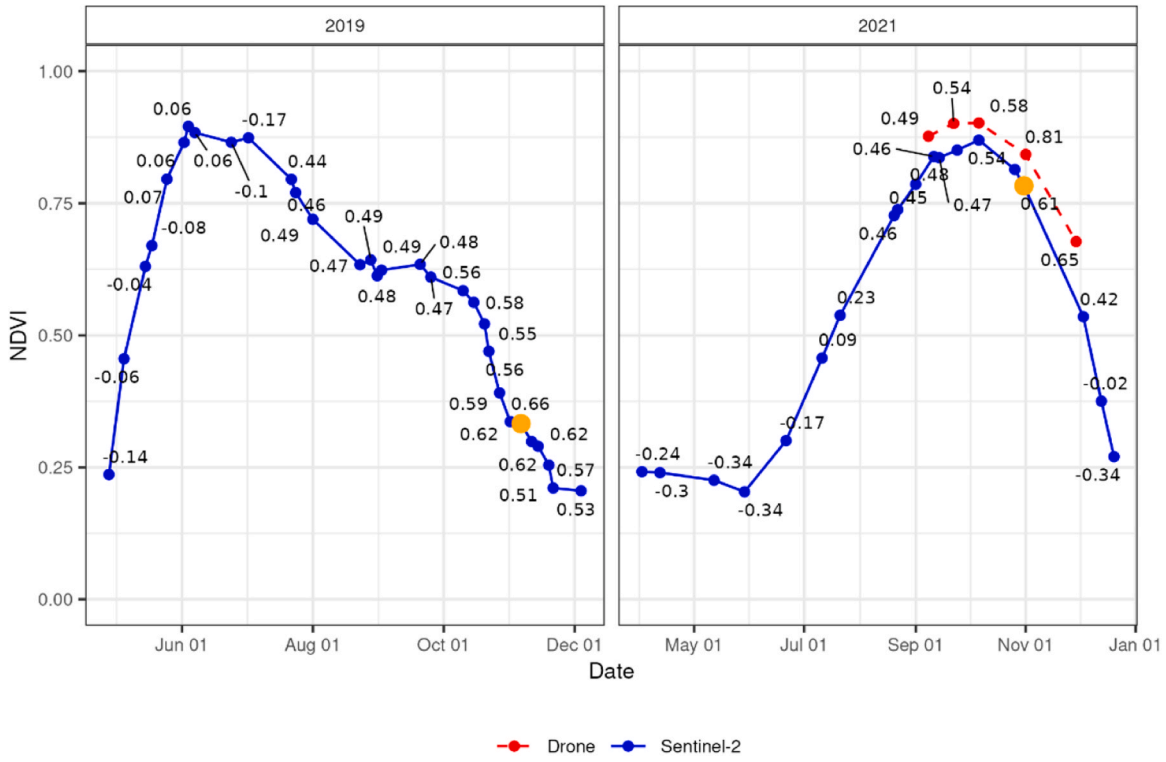

Fig. 4. Temporal dynamics of average NDVI from satellite (blue dots) and drone (red dots) sensing at full 10 ha field level in 2019 and 2021. The numbers are correlation coefficients of grid-level NDVI and yield maps at given dates. The spatial resolution of NDVI images from satellite and drone are 10 m x 10 m and 1 m x 1 m, respectively. The orange dots represent the date with the highest correlation coefficient.

harvester after the manual sampling, so data extracted from the yield map represents the average condition around the 1 m^2 point, while the crop samples on the exact location were removed manually. As these factors are difficult to avoid in the available yield maps and manual measurements, we need to keep this in mind when using this data at a fine resolution (e.g., 1 m^2).

For the LTT trial at BARS, our results show that 3 – 5 manual samples could produce an average yield value to represent the yield of a 1 ha strip, however, one sampling point for a 1/3 strip could not represent the sub-strip yield well. This further implies the need for replicates to offset the impact of spatial heterogeneity. The 30 sampling points in the LTT field were selected based on the heterogeneity evident in the digital soil maps. As yield maps reflect what the crop senses in the field, they may be effective, together with digital soil maps, to determine field zones and the number of measurements required across heterogeneous zones. Due to the difference in rooting depth, crop duration, and demands for water

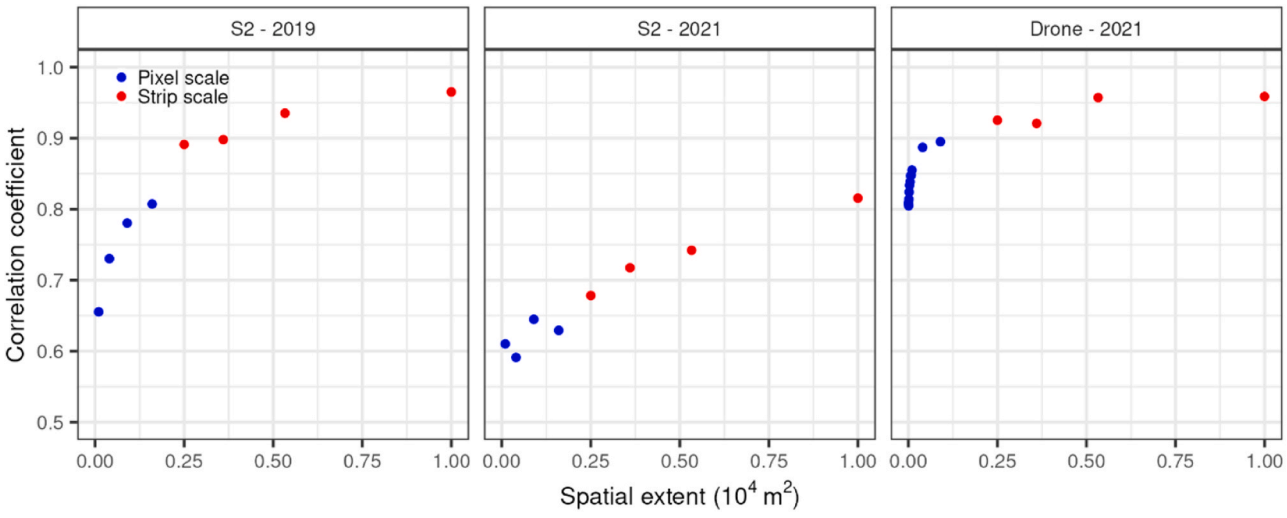

Fig. 5. The correlation coefficient between satellite/drone sensed NDVI and yield map at different spatial extents. The NDVI images on 6 Nov 2019 (Sentinel-2), 31 Oct 2021 (Sentinel-2) and 1 Nov 2021 (drone) were used as the highest spatial correlation between NDVI and yield occurred at these dates. The red dots indicate the coefficients at 1/4 strip, 1/3 strip, 1/2 strip and whole strip levels.

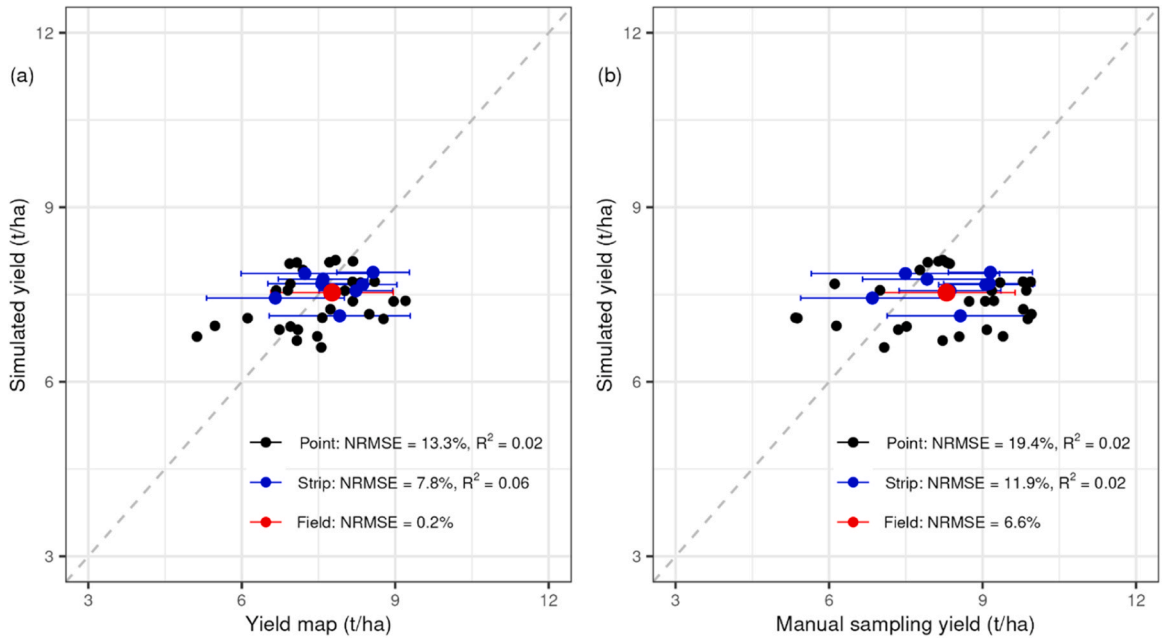

Fig. 6. Comparison of APSIM simulated wheat yield and those from yield map (a) and manual measurements (b) at point, strip and field scales. NRMSE is the normalized root mean square error between manually measured yield and yield map. R^2 is the coefficient of determination. Error bars represent the standard deviation of the sampling points.

and nutrients, the yield spatial variability of other crops may be different from wheat for a given field. For instance, differences in soil PAWC for different crop species have been noted even though limited data are available to characterise such differences (Verburg et al., 2021). We need to be mindful of this when utilizing such data with a detailed focus.

With the development of remote sensing technology, researchers are transitioning from destructive, time-consuming and labour-intensive sampling methods to non-destructive, high-throughput phenotyping techniques to estimate crop yield. A straightforward approach is to develop an empirical relationship between yield and remotely sensed vegetation indexes (VIs) or metrics derived from VI time series. Higher correlations between yield and VIs usually imply more accuracy for prediction. In this study, we found that aggregating fine resolution images to coarser resolution or larger spatial extent improved the correlation coefficient between remotely sensed NDVI (both satellite and drone) and yield maps for a given field, e.g., correlation coefficient increased from 0.66 to 0.89 when spatial resolution changed from 10 × 10 m pixel level to 0.25 ha 1/4 strip-level (satellite images of 2019). This was mainly due to many variances in the relationship between NDVI and yield at a finer resolution, and the variance was averaged out at larger pixel sizes or spatial extents (Figure S2). At a national scale, Deines et al. (2021) also demonstrated that satellite yield mapping accuracy with Landsat increased when spatial scales increased from pixel-level to county-level (R^2 increased from 0.40 to 0.69). Further work is warranted to investigate the usefulness of remote sensing data for yield predictions at different spatial scales (Donohue et al., 2018; Lobell et al., 2015; Maestrini and Basso, 2018; Ziliani et al., 2022).

NDVI derived from drone images had a higher correlation with yield

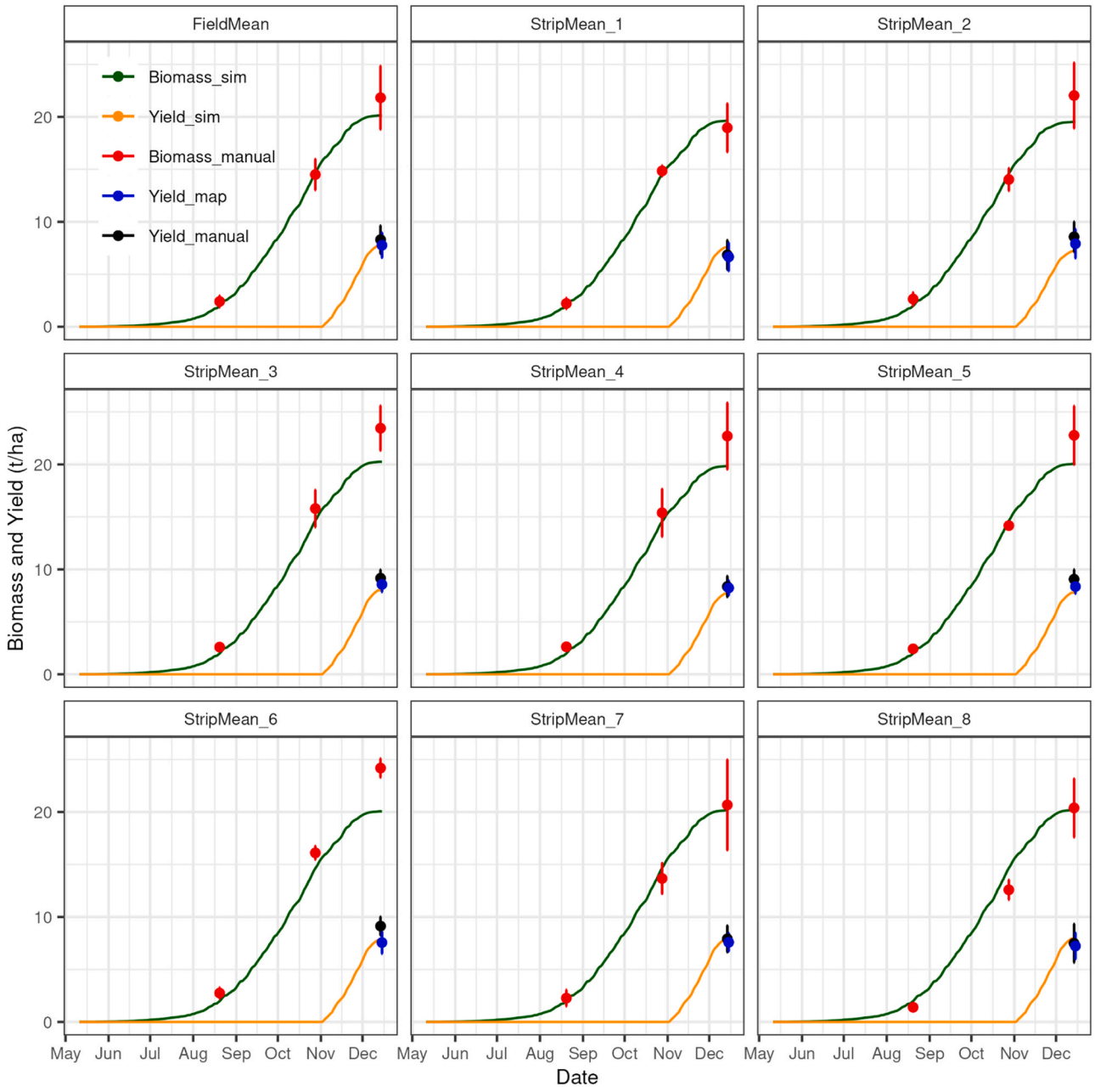

Fig. 7. Comparison of simulated biomass dynamics and grain yield of wheat compared to averages of manual measurements and yield map at strip and field scales. Error bars indicate the standard deviation.

maps than NDVI derived from satellite images at the same spatial resolution (Fig. 5). This is likely due to the greater detail provided by higher spatial resolution (4.24 × 4.24 cm) of the original drone images than satellite images (10 × 10 m). The ability of drones to acquire data close to the surface also reduces image contamination by clouds and atmosphere (Alvarez-Vanhard et al., 2021). This implies drone images may have more advantages than satellite images in field-scale applications. Synergising drone and satellite images may provide promising potential in applications across a range of spatial and temporal scales (Alvarez-Vanhard et al., 2021; Jiang et al., 2022).

Waldner et al. (2019) used an *in silico* approach based on crop modelling to explore which metrics derived from time series of the Leaf Area Index (LAI) achieve optimal performance in yield prediction across Australia. They found that integration of satellite observations from peak VI to harvest over time achieved better performance than single observation, e.g., peak VI. This was explained by the integration approach represents the intensity and the duration of the photosynthetic activity of the crop, which is highly correlated with measured yield. In this study, we calculated the correlation coefficients between yield and different types of metrics as well (data not shown), and interestingly, single observations at the later stage of crop growth had higher correlation than the peak value or integration metrics in the growing seasons of 2019 and 2021. Waldner et al. (2019) used a national scale dataset and predicted the yield across regions while our dataset focused on within-field yield variability. This demonstrates that different metrics or approaches may be needed when estimating yield at a sub-field or finer level (Maestrini and Basso, 2018; Ziliani et al., 2022).

In this study, the strongest correlation value between NDVI and yield maps varied across different years. Specifically, in 2019, the highest correlation was observed at the mid-grain filling stage, while in 2021, it was right after the flowering stage. This difference is likely caused by contrasting climatic conditions experienced during different wheat

developmental stages. The 2019 wheat was an early sown winter wheat and grew under a significant spring drought, while the 2021 wheat crop was a spring wheat was sown later and grew under much wetter conditions. The better rainfall conditions during 2021 enabled wheat to fill grains without water stress, with grain yield more closely related to the maximum LAI and NDVI than wheat in 2019. This indicates that the relationship between NDVI and yield maps for a given field would be time-specific and differs based on the year. The satellite image gap between 31 Oct 2021 and 3 Dec 2021 was due to the cloudy weather. The correlation coefficient during the missing data period may be higher than the one we currently identified.

Point-based simulations at BARS did not capture the spatial variability despite detailed initial soil condition, crop and management records. Statistical analysis showed no correlation between simulated/observed yield and soil water/nitrogen content. The possible reasons for such results include: (1) initial soil condition and PAWC may not be the key driver of crop yield in 2021; (2) other factors such as lateral flow of water and nutrients – which may be considerable due to the undulating terrain of the field. These factors may also contribute to the yield variability but are not captured by point-based APSIM simulations; (3) The same weather condition was used for all the points in the simulation, while local microclimate conditions particularly temperature variations related to slope could affect crop establishment and growth dynamics; (4) Unrepresentativeness and uncertainty of the soil input data at the point scale. The data from each sensor location/soil core provides useful information about the soil conditions (temperature, moisture, mineral N etc) at the particular point, these conditions may not reflect what the crop senses beyond that point. Nevertheless, the dataset used in this study is already the most detailed data that is available at present. It is important to keep in mind that applying process-based models at much finer scale would require more accurate inputs (soil, microclimate and management variations) at the matching scales and additional modelling of other impacts such as lateral flows of water and nutrients etc.

Despite the uncertainties at the point scale, APSIM modelling simulated the biomass dynamics and final wheat yields well at 1 ha strip- and 10 ha field scale. This result provides us confidence in APSIM-based modelling of crop growth and yield at an average field level, which is a powerful means to integrate and extend experimental results across seasons and investigate how soil and climate interactions affect land productivity and environmental performance in the long term. The better performance of the model predictions at the whole field scale also implies that model predictions for soil properties such as soil organic carbon may be better conducted at the whole field level for the purpose of calculating carbon credits.

One of the questions that arises from this study is - what spatial scales are needed for research and management purposes? For treatment layout of long-term experiments on a heterogeneous field, spatial variabilities in soil across the field must be considered for measurements and modelling, based on which zones can be delineated for representative measurements with replicates. One of the ideas of the LTT at BARS is to move away from replicated completely randomised block trials in the conventional way and instead to use digital technologies to embracing field variability (Kirkegaard et al., 2023). Modelling at matching scales can help integrate and extend experimental results and take account of the impact of soil variation, thus better reflecting the reality on farm and avoiding the need to restrict experiments to homogeneous fields. Sensing data at high spatial resolution may help with this. However, it remains unclear the degree to which detailed sensing and measurements at finer spatial resolutions could assist agronomic management of a heterogeneous field such as the LTT at BARS. For example, spatially explicit management practices of nitrogen fertilisation have been found to have relatively limited value (Robertson et al., 2008). Even modelling applications, productivity and environmental performance of cropping systems are more confidently evaluated at the whole field level.

5. Conclusion

With the advances in digital technologies, large amounts of spatial in-field data are becoming increasingly available to assist in research and farm management, which include manual measurements, crop yield maps, and remote/proximal sensing data at point or sub-field scales. This study reveals that data derived from remote/proximal sensing, yield maps, and manual measurements are poorly correlated at fine resolution (e.g., 1 m^2). However, when these point measurements are aggregated to coarse resolutions (e.g. >1 ha) correlation with spatial variation in crop performance is improved. The results from process-based modelling follows a similar trend and only becomes reliable at coarse resolutions at strip and field scale. Remotely sensed vegetation indices (VI) were correlated with yield map only when spatial resolution became coarse (> 50 m × 50 m), but the relationship and the timing of highest correlation differed between dry and wet years. The results highlight the need for caution when using yield maps and remote sensing data to estimate yield and quantify spatial variability at a fine resolution (e.g., 1 m^2).

CRediT authorship contribution statement

Eusun Han: Writing – review & editing, Writing – original draft, Investigation, Formal analysis, Data curation. **John Kirkegaard:** Writing – review & editing, Writing – original draft, Project administration, Investigation, Data curation. **Tony Swan:** Writing – review & editing, Project administration, Investigation, Data curation. **Brendan Malone:** Writing – review & editing, Writing – original draft, Investigation, Formal analysis, Data curation. **Julianne Lilley:** Writing – review & editing, Project administration, Investigation. **Enli Wang:** Writing – review & editing, Writing – original draft, Supervision, Methodology, Formal analysis, Conceptualization. **Di He:** Writing – review & editing, Writing – original draft, Visualization, Methodology, Investigation, Formal analysis, Data curation, Conceptualization. **Stuart Brown:** Writing – review & editing, Project administration, Data curation. **Roger Lawes:** Writing – review & editing, Investigation. **Mark Glover:** Writing – review & editing, Investigation, Data curation.

Declaration of Competing Interest

The authors declare that they have no known competing financial interests or personal relationships that could have appeared to influence the work reported in this paper.

Data Availability

Data will be made available on request.

Appendix A. Supporting information

Supplementary data associated with this article can be found in the online version at doi:10.1016/j.fcr.2024.109332.

References

Alvarez-Vanhard, E., Corpetti, T., Houet, T., 2021. UAV & satellite synergies for optical remote sensing applications: a literature review. Sci. Remote Sens. 3, 100019 https://doi.org/10.1016/j.srs.2021.100019.

Batchelor, W.D., Basso, B., Paz, J.O., 2002. Examples of strategies to analyze spatial and temporal yield variability using crop models. Eur. J. Agron. Process Simul. Appl. Crop. Syst. Models 18, 141–158. https://doi.org/10.1016/S1161-0301(02)00101-6.

Boenecke, E., Lueck, E., Ruehlmann, J., Gruendling, R., Franko, U., 2018. Determining the within-field yield variability from seasonally changing soil conditions. Precis. Agric. 19, 750–769. https://doi.org/10.1007/s11119-017-9556-z.

Bölenius, E., Stenberg, B., Arvidsson, J., 2017. Within field cereal yield variability as affected by soil physical properties and weather variations – a case study in east central Sweden. Geoderma Reg. 11, 96–103. https://doi.org/10.1016/j.geodrs.2017.11.001.

Campos, I., González-Gómez, L., Villodre, J., Calera, M., Campoy, J., Jiménez, N., Plaza, C., Sánchez-Prieto, S., Calera, A., 2019. Mapping within-field variability in wheat yield and biomass using remote sensing vegetation indices. Precis. Agric. 20, 214–236. https://doi.org/10.1007/s11119-018-9596-z.

Coughlan, K., Cresswell, H., McKenzie, N., 2002. Soil Physical Measurement and Interpretation for Land Evaluation. CSIRO Publishing. ⟨https://www.publish.csiro.au/book/3147⟩.

Deines, J.M., Patel, R., Liang, S.-Z., Dado, W., Lobell, D.B., 2021. A million kernels of truth: Insights into scalable satellite maize yield mapping and yield gap analysis from an extensive ground dataset in the US Corn Belt. Remote Sens. Environ. 253, 112174 https://doi.org/10.1016/j.rse.2020.112174.

Donohue, R.J., Lawes, R.A., Mata, G., Gobbett, D., Ouzman, J., 2018. Towards a national, remote-sensing-based model for predicting field-scale crop yield. Field Crops Res. 227, 79–90. https://doi.org/10.1016/j.fcr.2018.08.005.

Gaso, D.V., de Wit, A., Berger, A.G., Kooistra, L., 2021. Predicting within-field soybean yield variability by coupling Sentinel-2 leaf area index with a crop growth model. Agric. For. Meteorol., 108553 https://doi.org/10.1016/j.agrformet.2021.108553.

Godwin, R.J., Miller, P.C.H., 2003. A review of the technologies for mapping within-field variability. Biosyst. Eng. Precis. Agric. - Manag. Soil Crop Var. Cereals 84, 393–407. https://doi.org/10.1016/S1537-5110(02)00283-0.

Gorelick, N., Hancher, M., Dixon, M., Ilyushchenko, S., Thau, D., Moore, R., 2017. Google Earth Engine: Planetary-scale geospatial analysis for everyone. Remote. Sens. Environ. Big Remote. Sense Data: tools, Appl. Exp. 202, 18–27. https://doi.org/10.1016/j.rse.2017.06.031.

He, D., Wang, E., 2019. On the relation between soil water holding capacity and dryland crop productivity. Geoderma 353, 11–24. https://doi.org/10.1016/j.geoderma.2019.06.022.

He, D., Oliver, Y., Wang, E., 2021. Predicting plant available water holding capacity of soils from crop yield. Plant Soil 459, 315–328. https://doi.org/10.1007/s11104-020-04757-0.

He, D., Oliver, Y., Rab, A., Fisher, P., Armstrong, R., Kitching, M., Wang, E., 2022. Plant available water capacity (PAWC) of soils predicted from crop yields better reflects within-field soil physicochemical variations. Geoderma 422, 115958. https://doi.org/10.1016/j.geoderma.2022.115958.

Hijmans, R.J., Bivand, R., Pebesma, E., Sumner, M.D., 2023. terra: Spatial Data Analysis.

Holzworth, D.P., Huth, N.I., deVoil, P.G., Zurcher, E.J., Herrmann, N.I., McLean, G., Chenu, K., van Oosterom, E.J., Snow, V., Murphy, C., Moore, A.D., Brown, H., Whish, J.P.M., Verrall, S., Fainges, J., Bell, L.W., Peake, A.S., Poulton, P.L., Hochman, Z., Thorburn, P.J., Gaydon, D.S., Dalgliesh, N.P., Rodriguez, D., Cox, H., Chapman, S., Doherty, A., Teixeira, E., Sharp, J., Cichota, R., Vogeler, I., Li, F.Y., Wang, E., Hammer, G.L., Robertson, M.J., Dimes, J.P., Whitbread, A.M., Hunt, J., van Rees, H., McClelland, T., Carberry, P.S., Hargreaves, J.N.G., MacLeod, N., McDonald, C., Harsdorf, J., Wedgwood, S., Keating, B.A., 2014. APSIM – Evolution towards a new generation of agricultural systems simulation. Environ. Model. Softw. 62, 327–350. https://doi.org/10.1016/j.envsoft.2014.07.009.

Hu, P., Chapman, S.C., Jin, H., Guo, Y., Zheng, B., 2021. Comparison of modelling strategies to estimate phenotypic values from an unmanned aerial vehicle with spectral and temporal vegetation indexes. Remote Sens. 13, 2827. https://doi.org/10.3390/rs13142827.

Huggins, D.R., Alderfer, R.D., 1995. Yield variability within a long-term corn management study: implications for precision farming. In: Site-Specific Management for Agricultural Systems. John Wiley & Sons, Ltd, pp. 417–426. https://doi.org/10.2134/1995.site-specificmanagement.c28.

Isbell, R., 2021. The Australian Soil Classification. CSIRO Publishing.

Jiang, J., Johansen, K., Tu, Y.-H., McCabe, M.F., 2022. Multi-sensor and multi-platform consistency and interoperability between UAV, Planet CubeSat, Sentinel-2, and Landsat reflectance data. GIScience Remote Sens. 59, 936–958. https://doi.org/10.1080/15481603.2022.2083791.

Jin, X., Kumar, L., Li, Z., Feng, H., Xu, X., Yang, G., Wang, J., 2018. A review of data assimilation of remote sensing and crop models. Eur. J. Agron. 92, 141–152. https://doi.org/10.1016/j.eja.2017.11.002.

Jones, E.J., Bishop, T.F.A., Malone, B.P., Hulme, P.J., Whelan, B.M., Filippi, P., 2022. Identifying causes of crop yield variability with interpretive machine learning. Comput. Electron. Agric. 192, 106632 https://doi.org/10.1016/j.compag.2021.106632.

Jordan, C., Shi, Z., Bailey, J.S., Higgins, A.J., 2003. Sampling strategies for mapping 'within-field' variability in the dry matter yield and mineral nutrient status of forage grass crops in cool temperate climes. Precis. Agric. 4, 69–86. https://doi.org/10.1023/A:1021815122216.

Keating, B.A., Carberry, P.S., Hammer, G.L., Probert, M.E., Robertson, M.J., Holzworth, D., Huth, N.I., Hargreaves, J.N.G., Meinke, H., Hochman, Z., McLean, G., Verburg, K., Snow, V., Dimes, J.P., Silburn, M., Wang, E., Brown, S., Bristow, K.L., Asseng, S., Chapman, S., McCown, R.L., Freebairn, D.M., Smith, C.J., 2003. An overview of APSIM, a model designed for farming systems simulation. Eur. J. Agron. Model. Crop. Syst.: Sci. Softw. Appl. 18, 267–288. https://doi.org/10.1016/S1161-0301(02)00108-9.

Kharel, T.P., Swink, S.N., Maresma, A., Youngerman, C., Kharel, D., Czymmek, K. j, Ketterings, Q.M., 2019. Yield monitor data cleaning is essential for accurate corn grain and silage yield determination. Agron. J. 111, 509–516. https://doi.org/10.2134/agronj2018.05.0317.

Kirkegaard J., Malone B., Glover M., Han E., Brown S., Richardson A., Swan T., Wang E., He D., Moloney J., 2023. A contemporary long-term farming systems experiment for the digital age. In: Long Term Experiments: Meeting future Challenges, Rothamsted 20-22 June, Association of Applied Biologists Abstract Booklet pp 6.

Kosmowski, F., Chamberlin, J., Ayalew, H., Sida, T., Abay, K., Craufurd, P., 2021. How accurate are yield estimates from crop cuts? Evidence from smallholder maize farms in Ethiopia. Food Policy 102, 102122. https://doi.org/10.1016/j.foodpol.2021.102122.

Lobell, D.B., Thau, D., Seifert, C., Engle, E., Little, B., 2015. A scalable satellite-based crop yield mapper. Remote Sens. Environ. 164, 324–333. https://doi.org/10.1016/j.rse.2015.04.021.

Lai, Y.R., Pringle, M.J., Kopittke, P.M., Menzies, N.W., Orton, T.G., Dang, Y.P., 2018. An empirical model for prediction of wheat yield, using time-integrated Landsat NDVI. International Journal of Applied Earth Observation and Geoinformation 72, 99–108. https://doi.org/10.1016/j.jag.2018.07.013.

Maestrini, B., Basso, B., 2018. Predicting spatial patterns of within-field crop yield variability. Field Crop. Res. 219, 106–112. https://doi.org/10.1016/j.fcr.2018.01.028.

Malone, B., Stockmann, U., Glover, M., McLachlan, G., Engelhardt, S., Tuomi, S., 2022. Digital soil survey and mapping underpinning inherent and dynamic soil attribute condition assessments. Soil Secur. 6, 100048 https://doi.org/10.1016/j.soisec.2022.100048.

Minasny, B., McBratney, A.B., 2006. A conditioned Latin hypercube method for sampling in the presence of ancillary information. Comput. Geosci. 32, 1378–1388. https://doi.org/10.1016/j.cageo.2005.12.009.

Pettorelli, N., Vik, J.O., Mysterud, A., Gaillard, J.-M., Tucker, C.J., Stenseth, N.Chr, 2005. Using the satellite-derived NDVI to assess ecological responses to environmental change. Trends Ecol. Evol. 20, 503–510. https://doi.org/10.1016/j.tree.2005.05.011.

R Core Team, 2022. R: a language and environment for statistical computing [WWW Document]. URL ⟨https://www.gbif.org/tool/81287/r-a-language-and-environment-for-statistical-computing⟩ (accessed 8.4.23).

Ratcliff, C., Gobbett, D., Bramley, R., 2019. PAT: Accessible tools for precision agriculture data analysis, in: Proceedings of the 2019 Agronomy Australia Conference. p. 4.

Robertson, M.J., Lyle, G., Bowden, J.W., 2008. Within-field variability of wheat yield and economic implications for spatially variable nutrient management. Field Crop. Res. 105, 211–220. https://doi.org/10.1016/j.fcr.2007.10.005.

Skakun, S., Kalecinski, N.I., Brown, M.G.L., Johnson, D.M., Vermote, E.F., Roger, J.-C., Franch, B., 2021. Assessing within-field corn and soybean yield variability from WorldView-3, Planet, Sentinel-2, and Landsat 8 satellite imagery. Remote Sens. 13, 872. https://doi.org/10.3390/rs13050872.

Stock, W.D., 1983. An evaluation of some manual colorimetric methods for the determination of inorganic nitrogen in soil extracts. Commun. Soil Sci. Plant Anal. 14, 925–936. https://doi.org/10.1080/00103628309367420.

Taylor, S.L., Payton, M.E., Raun, W.R., 1999. Relationship between mean yield, coefficient of variation, mean square error, and plot size in wheat field experiments. Commun. Soil Sci. Plant Anal. 30, 1439–1447. https://doi.org/10.1080/00103629909370298.

Verburg, K., Li, X., Deery, D., Schwenke, G., Poulton, P., Wasson, A., Kirkegaard, J., Dang, Y., Sandral, G., Bell, L., 2021. Plant Available Water Capacity – crop and varietal differences in soil water extraction. GRDC.

Waldner, F., Horan, H., Chen, Y., Hochman, Z., 2019. High temporal resolution of leaf area data improves empirical estimation of grain yield. Sci. Rep. 9, 15714 https://doi.org/10.1038/s41598-019-51715-7.

Zadoks, J.C., Chang, T.T., Konzak, C.F., 1974. A decimal code for the growth stages of cereals. Weed Res. 14, 415–421.

Zarco-Tejada, P.J., Ustin, S.L., Whiting, M.L., 2005. Temporal and spatial relationships between within-field yield variability in cotton and high-spatial hyperspectral remote sensing imagery. Agron. J. 97, 641–653. https://doi.org/10.2134/agronj2003.0257.

Zhao, Z., Wang, E., Kirkegaard, J.A., Rebetzke, G.J., 2022. Novel wheat varieties facilitate deep sowing to beat the heat of changing climates. Nat. Clim. Change 12, 291–296. https://doi.org/10.1038/s41558-022-01305-9.

Ziliani, M.G., Altaf, M.U., Aragon, B., Houborg, R., Franz, T.E., Lu, Y., Sheffield, J., Hoteit, I., McCabe, M.F., 2022. Early season prediction of within-field crop yield variability by assimilating CubeSat data into a crop model. Agric. For. Meteorol. 313, 108736 https://doi.org/10.1016/j.agrformet.2021.108736.